Synthesis and Characterization of Ethyl Methacrylate–Acrylamide Copolymers

B. SRINIVASULU, P. RAGHUNATH RAO,* and E. V. SUNDARAM

Department of Chemistry, Kakatiya University, Warangal-506 009, India

SYNOPSIS

Free radical copolymerization of ethyl methacrylate (EMA) and acrylamide (AA) was carried out in the presence of 2,2′-azobisisobutyronitrile (AIBN) in dimethyl formamide (DMF) at 60°C. The percentage composition of the copolymers were established by elemental analysis. The copolymerization reactivity ratios were determined by both Fineman–Ross (F-R) and Kelen–Tudos (K–T) methods. The copolymers were characterized by IR, ^{1}H-NMR, thermal, and dielectric studies. Glass transition temperatures (T_g) have been determined by DSC. The solubility parameter of this copolymer was evaluated by studying the intrinsic viscosity in different solvents.

INTRODUCTION

Acrylic copolymers have acquired prime importance in various avenues of industrial applications.[1-3] They serve as basic materials for the preparation of formulations that are used as base and top coats in leather industry. Saini et al.[4] studied the free radical copolymerization of acrylamide (AA)–methyl methacrylate and AA–styrene. Copolymerization of acrylamide with styrene,[5] *n*-butyl acrylate,[6] acrylic acid,[7] methyl vinyl ketone,[8] acrylo nitrile,[9] and methacrylic acid[10] were also studied by various workers in the past few years. In our earlier paper,[11] we determined the reactivity ratios of methacrylamide with ethyl methacrylate (EMA). In the present investigation, reactivity ratios, thermal electrical properties, and solubility parameters of EMA–AA copolymer systems are studied.

EXPERIMENTAL

Ethyl methacrylate (Fluka) was purified from inhibitor by washing with 5% sodium hydroxide in water, and dried over calcium chloride and distilled twice under reduced pressure. Acrylamide was crystallized from chloroform. 2,2′-Azobisisobutyronitrile (AIBN) (Fluka) was crystallized from methanol. *N,N*-Dimethyl formamide (DMF) (Qualigens) was reagent grade product and was dried and purified by distillation before use.

All experiments were performed in glass tubes filled with dry monomers, solvents, and initiator. The tubes were then sealed in a nitrogen atmosphere and introduced into the thermostat at desired temperature. The reaction was allowed to go for less than 10% conversion, the reactions were stopped by adding excess volume of water as nonsolvent, and the copolymers were precipitated, washed thoroughly with ether and hexane to remove DMF and unreacted monomer. Reprecipitation was done from acetone solution. The total concentration was kept constant at (1.6 mol/L monomers). The initiator was used at 0.6 g/L solvent.

The IR spectra of the copolymers were recorded with Perkin-Elmer model spectrophotometer.

^{1}H-NMR spectra were recorded from $CDCl_3$ solution using a EM-360 60 MHz spectrometer. The glass transition temperatures, T_g, of the copolymers were determined by differential scanning calorimetry (DSC) at a heating rate of 8°C/min. Thermogravimetric analysis (TGA) was carried out using a Dupont 900 thermobalance in air at a heating rate of 8°C/min.

The integral procedural decomposition temperature (IPDT)[12] values were determined from a

* To whom correspondence should be addressed.

Journal of Applied Polymer Science, Vol. 43, 1521–1525 (1991)
 CCC 0021-8995/91/081521-05$04.00

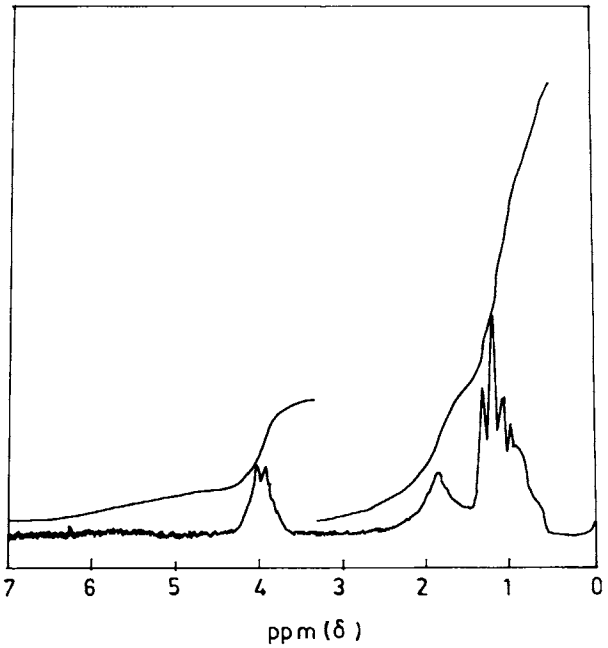

Figure 1 ^{1}H-NMR spectrum of EMA–AA copolymer.

mass-loss curve. The curve was divided into small squares. The area under the curve was integrated by weighing a paper of the curve on an analytical balance. The mass of the cross-hatched region divided by the mass of the total rectangular plotting area was the total curve area, A^*, normalized with respect to both residual mass and temperature. The quantity A^* is converted to a temperature T_A^*:

$$T_A^* = 875A^* + 25, \qquad (1)$$

where T_A^* represents a characteristic end-of-volatilisation temperature. Doyle showed that the product A^*K^* represented a comprehensive index of intrinsic thermal stability by substituting A^*K^* for A^* in eq. (1). K^* is the ratio between the doubly cross-hatched area and the rectangular area bounded by the characteristic end-of-volatilisation temperature.

$$\text{IPDT} = 875A^*K^* + 25. \qquad (2)$$

The AA content of the copolymer samples are determined by Carlo-Erba Model 1106 elemental analyzer to obtain data on the copolymer composition. The copolymer compositions were ascertained from the AA content in the copolymers. The reactivity ratio values for this system was estimated by Fineman–Ross[13] and Kelen–Tudos[14] methods.

Dielectric measurements were made with GR 1620 A capacitance bridge in the frequency range 10^2–10^5 Hz and temperature range 30–110°C. Polymer samples are taken in the form of pellets pressed at a constant pressure. Aluminum foils are used on either side of the samples to ensure good contact and to remove the air gaps between the sample and electrodes. The samples are dried before making measurements. Temperature is measured using a copper constantan thermocouple and a digital panelmeter.

For determination of solubility parameter, the viscosities were measured using a suspended level dilution viscometer of ubbelohde type. The intrinsic viscosity $[\eta]$ was evaluated at a single concentration (1%) from the flow time of pure solvent (t_0) and the solution (t) by the relationship[15–17]:

$$[\eta] = [2(t/t_0 - \text{Ln}(t/t_0) - 1)]^{1/2}\, 1/C,$$

where C is the concentration in g/dL.

RESULTS AND DISCUSSION

The IR spectra of the copolymers show a strong band at 1,740 cm^{-1} due to carbonyl in ester groups and a

Table I Copolymerization of EMA–AA

Run	Mol Ratio in Feed [EMA]/[AA]	N%	Copolymer Composition [EMA] Mol %	Copolymer Composition [AA] Mol %	T_g (°C)
1	1.686	2.26	82.7	17.2	76
2	1.024	3.02	77.5	22.4	79
3	0.857	3.32	75.4	24.5	81
4	0.743	3.82	72.2	27.8	83
5	0.542	5.12	63.9	36.1	90

Temperature, 60 ± 1°C; AIBN, 0.6 g/L.

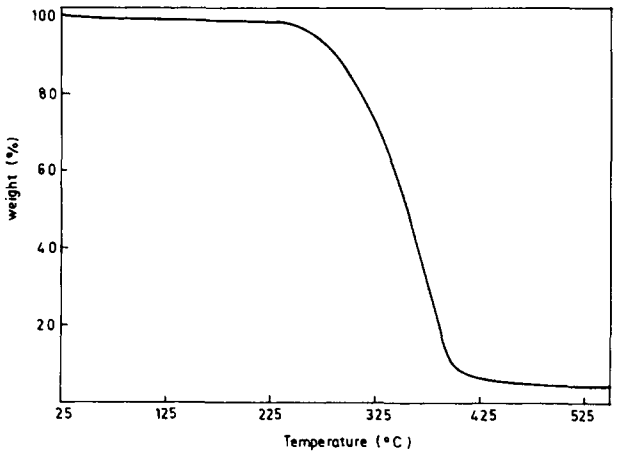

Figure 2 TGA of EMA–AA copolymer (feed ratio 1.024).

strong band at 2,950 cm^{-1} from C—H stretching. The strong band at 1,640 cm^{-1} is due to carbonyl in amide groups and 3,400–3,500 cm^{-1} is due to —NH— stretching vibrations.

^{1}H-NMR spectrum of EMA–AA copolymer is given in Figure 1. In ^{1}H-NMR, $-OCH_2$ protons of ethyl methacrylate appear at 3.7–4.3 ∂. β-Methylene protons appear in the region of 1.6–2.1 ∂, and α-methyl protons and CH_3— protons of alkyl part of ester appear in the region of 0.9–1.3 ∂. Amide protons of acrylamide appeared at 5.0–6.3 ∂. These signals, characteristic of both monomers, clearly showed their presence in the copolymer.

The composition of the copolymers formed with varying feed composition was determined by nitrogen estimation (Table I). This datum was used for the evaluation of reactivity ratios of EMA–AA system by F–R and K–T methods.

The values of r_1 (EMA) and r_2 (AA) so obtained were 2.70 ± 0.01 and 0.11 ± 0.01 by F–R and 2.74 ± 0.02 and 0.12 ± 0.015 by K–T methods. For this system, the value of r_1 is more than one, whereas r_2 is less than one. The product of r_1 and r_2 remains less than unity, indicating that the copolymers are weakly ordered with a predominantly random distribution of the monomeric units in the polymer chain. The high value of r_1 indicates that the probability of EMA entering into the copolymer chain is higher than that of AA. The copolymer formed is therefore richer in ethyl methacrylate.

Table II Thermogravimetric Analysis of EMA–AA Copolymers

Mol Ratio in Feed [EMA]/[AA]	DT (°C)	IPDT (°C)	Temperature (°C) at Wt. Loss 10%	20%	60%
1.024	239	466.64	284	312.5	365
0.857	255	494.65	302	327.5	372
0.743	260	504.88	305	330.0	375

The glass transition temperatures (T_g) of copolymer systems increased with an increase in acrylamide content (Table I) in the copolymer. The route cause for such an increase is probably due to increased intermolecular interactions of amide group.

A thermogram of EMA–AA copolymer is given in Figure 2. TGA of the copolymer showed a single-stage weight loss. The results of IPDT and the decomposition temperature for various copolymer compositions are summarized in Table II. Since IPDT value is a measure of thermal stability of a polymer, it is evident from the data that the IPDT value increases with an increasing content of AA in the copolymers results in an increase in thermal stability. As the acrylamide content increases, the decomposition temperature also increases at varying percentage of weight loss.

Typical plot of ϵ and tan ∂ against temperature for composition 2 (Fig. 3) shows that initially ϵ and tan ∂ are unaffected by temperature up to 60°C. Beyond that region, both ϵ and tan ∂ increase. A peak due to relaxation is observed in tan ∂, known as α-relaxation, at 95°C in the rubbery state of polymer.[18,19] This temperature is higher than the glass transition temperature for the polymer obtained by

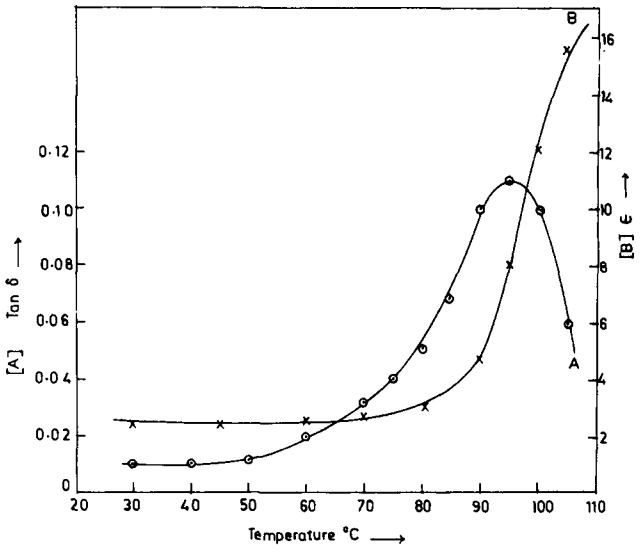

Figure 3 Typical plot of tan ∂ and ϵ vs. temperature.

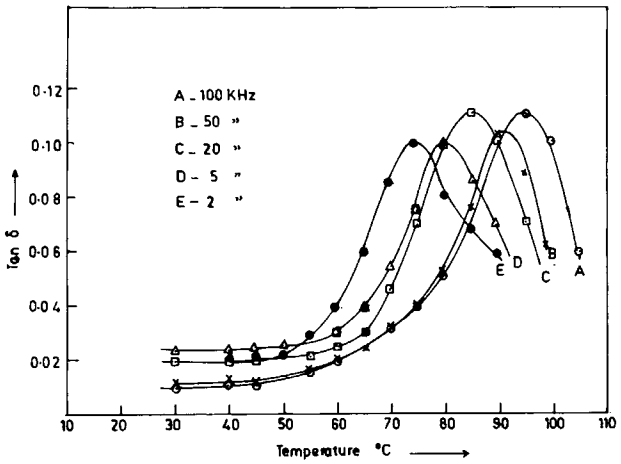

Figure 4 Plot of tan ∂ vs. temperature at different frequencies.

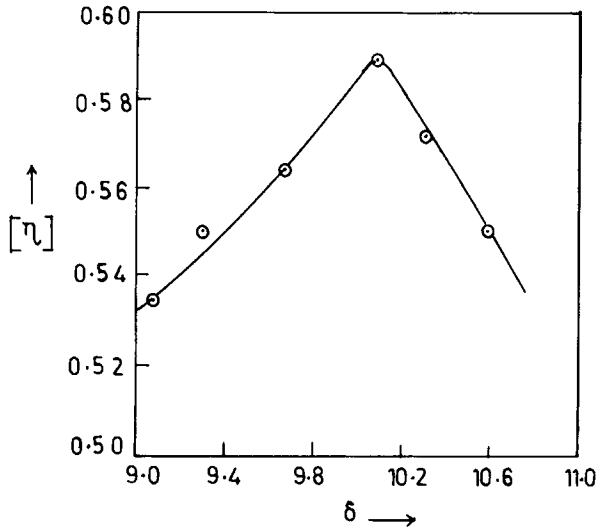

Figure 5 Plot of $[\eta]$ vs. ∂.

any static method. At lower temperatures, molecular chains are not only immobile but also tightly bound at some points due to dipole–dipole interactions.[20] As the temperature is increased, more dipole groups are released and the mobility of polymer segments increases.

Variation of tan ∂ with temperature for copolymer composition 2 was studied at five different frequencies, namely, 2, 5, 20, 50, and 100 KHz (Fig. 4). Tan ∂ is found to shift toward higher temperatures with increase in the frequency. The absorption maxima are observed at 75, 80, 85, 91, and 95°C for frequencies 2, 5, 20, 50, and 100 KHz, respectively.

Solubility Parameter of Copolymer

Analytical reagent grade solvents with solubility parameters in the range of 9.1–10.6 $(cal/cm^3)^{1/2}$ were selected for viscosity measurements. The composition of the copolymer used was (77.5 : 22.4). The intrinsic viscosity $[\eta]$ and their dependence on solubility parameter ∂ of solvents are given in Table III. The solubility parameter[21–23] of polymer was determined by measuring the intrinsic viscosity of the polymer in different solvents. Then the intrinsic viscosity was plotted against the solubility parameter of the several solvents. Since chain conformation is most expanded in the best solvent, the intrinsic viscosity will be highest for the best match in solubility parameter.

In the present study, the dependence of intrinsic viscosity on the solubility parameter of solvents has been used for estimating solubility parameter of the copolymer. The intrinsic viscosity of the copolymer solution attains optimum value when solubility parameter of the copolymer falls in the vicinity of that of the solvent ∂_p. The solubility parameter of the copolymer has been estimated by equating it to that of the solvent at which $[\eta]$ has the maximum value in the plot $[\eta]$ vs. ∂ (Fig. 5).

The estimated value for this copolymer was 10.1 $(cal/cm^3)^{1/2}$ or $[20.7\ (J/m^3)^{1/2}\ 10^3]$.

Table III Intrinsic Viscosities $[\eta]$ and Their Dependence on Solubility Parameter ∂ of Solvents

		Solubility Parameter	EMA–AA Copolymer
No.	Solvent	∂ $(cal/cm^3)^{1/2}$	$[\eta]$ in dL/g
1	Tetrahydrofuran	9.1	0.535
2	Chloroform	9.3	0.550
3	Methylene chloride	9.7	0.564
4	Acetic acid	10.1	0.589
5	Acetic anhydride	10.3	0.572
6	Diethyl formamide	10.6	0.551

CONCLUSIONS

In conclusion, we can state that T_g values and thermal stability have been found to increase with an increase in the content of acrylamide in the copolymer. The dielectric constant and loss factor were found to be temperature dependent. Tan ∂_{max} of these copolymers were found to shift toward higher temperatures with increase in the frequency of the electric fields.

The authors are thankful to U.G.C., New Delhi, for financial assistance under a major research project. One of the authors (B.S.) thanks the CSIR, New Delhi, for awarding him as Senior Research Fellow.

REFERENCES

1. F. Payne, *Organic Coating Technology,* John Wiley, New York, 1964, vol. 1, p. 536.
2. C. R. Martens, *Technology of Paints, Varnishes and Lacquers,* Reinhold, New York, 1968, p. 111.
3. H. Warson, *The Application of Synthetic Resin Emulsions,* Ernest Benn, London, 1972, p. 215.
4. G. Saini, A. Leoni, and S. Franco, *Makromol. Chem.,* **144,** 235 (1971).
5. C. I. Simionescu, K. C. Suk, S. Dumitriu, E. Comanita, and M. Pastravanu, *Polym. Bull.,* **15**(6), 503 (1986).
6. T. R. Balasubramanian and V. Mahadevan, *J. Macromol. Sci. Chem.,* **A21,** 245 (1984).
7. S. K. Malhotra and D. Yadav, *J. Polym. Sci., Poly. Chem. Ed.,* **22**(12), 3697 (1984).
8. N. Yamashita, K. Ikezawa, S. I. Ayukawa, and T. Maeshima, *J. Macromol. Sci. Chem.,* **A21**(5), 621 (1984).
9. S. N. Bhadani, and K. Swapna, *Makromol. Chem. Rapid Commun.,* **1**(4), 281 (1980).
10. D. A. Topchiev, V. Z. Shakirov, L. P. Kalinina, T. M. Karaputadze, and V. A. Kavanov, *Vysokomolekul. Soedin, A.,* **14,** 581 (1972).
11. B. Srinivasulu, P. Raghunath Rao, and E. V. Sundaram, *J. Poly. Mater.,* **7,** 77 (1990).
12. C. D. Doyle, *Anal. Chem.,* **33,** 77 (1961).
13. M. Fineman and S. D. Ross, *J. Polym. Sci.,* **5,** 259 (1950).
14. T. Kelen and F. Tudos, *J. Macromol. Sci. Chem.,* **A9,** 1 (1975).
15. O. F. Solomon and I. Z. Ciuta, *J. Appl. Polym. Sci.,* **6,** 683 (1962).
16. R. Z. Near, N. H. Zabwsky, and R. F. Hettmiller, *J. Appl. Polym. Sci.,* **7,** 830 (1963).
17. M. M. Zafar and R. Mahmood, *Makromol. Chem.,* **175,** 903 (1974).
18. A. Adam, *Koll. Zeitschr. Zeitschr. Polym.,* **180,** 11 (1962).
19. A. Tanaka and Y. Ishida, *J. Phys. Soc. Jpn.,* **15,** 161 (1960).
20. A. K. Gupta, R. P. Singhal, and V. R. Agarwal, *Polymer,* **22,** 285 (1981).
21. M. V. Ram Mohan and M. Yaseen, *J. Coat. Tech.,* **58**(743), 49 (1986).
22. H. G. Elias, *Makromol. Chem.,* **180,** 1243 (1979).
23. K. M. A. Shareef and M. Yaseen, *J. Coat. Tech.,* **55**(701), 48 (1983).

Received July 30, 1990
Accepted January 2, 1991